

Description and molecular phylogeny of *Paramecium grohmannae* sp. nov. (Ciliophora, Peniculida) from a wastewater treatment plant in Brazil

Thiago da Silva Paiva^{1,2,*}, Bárbara do Nascimento Borges³, Maria Lúcia Harada² & Inácio Domingos da Silva-Neto⁴

¹Laboratory of Evolutionary Protistology, Instituto de Biociências, Universidade de São Paulo.

²Laboratório de Biologia Molecular “Francisco Mauro Salzano”, Instituto de Ciências Biológicas, Universidade Federal do Pará

³Centro de Tecnologia Agropecuária, Instituto Socioambiental e dos Recursos Hídricos, Universidade Federal Rural da Amazônia

⁴Laboratório de Protistologia, Departamento de Zoologia, Instituto de Biologia, CCS, Universidade Federal do Rio de Janeiro

*Corresponding author: tpaiva@biologia.ufrj.br

Abstract. A new morphological species of *Paramecium* Müller, 1773, was discovered in samples of water with activated sludge of a wastewater treatment plant in Rio de Janeiro, Brazil. It is described based on light microscopy and its phylogenetic position hypothesized from 18S-rDNA analyses. *Paramecium grohmannae* sp. nov. is characterized by a unique combination of features. It is a counterclockwise rotating freshwater *Paramecium* with body outline intermediate between “aurelia” and “bursaria” forms, two contractile vacuoles, each with one excretion pore and usually nine collecting canals; oral opening slight below body equator; macronucleus ellipsoid to obovoid, measuring ~64 x 24 µm and located in anterior half of body; one (less frequently two) globular endosomal micronuclei ~5 µm in diameter with endosome ~2.5 µm. Phylogenetic analyses unambiguously place the new species within the *P. multimicronucleatum* complex.

Keywords: activated sludge, ciliate, Oligohymenophorea, Protista, South America.

INTRODUCTION

Ciliates are microscopic eukaryotes found in most of the world habitats, occurring in soils, freshwater and marine environments, and participating in microbial food webs as bacterial grazers and predators of other protists and small metazoans (FENCHEL, 1987; LYNN, 2008). As result, ciliates are important for the water industry because they can accelerate the process of water clarification by

consuming bacteria, and their identification and quantification permit to rapidly assess water quality (CURDS & COCKBURN, 1970; AL-SHAHWANI & HORAN, 1991; CURDS, 1992; SILVA & SILVA-NETO, 2001).

Among ciliates, *Paramecium* Müller, 1773, is one of the most well-known organisms, serving as experimental model for a wide array of studies (see BEALE, 1954; VAN WAGTENDONK, 1974; GÖRTZ, 1988; BEALE & PREER-JR, 2008). Currently, there are more than 40 species of *Paramecium* described in

the literature (FOKIN & CHIVILEV 2000; FOKIN, 2010), albeit in a recent review of the main morphotypes, FOKIN (2010) recognized 17 valid species. This number, however, can increase with reassessment of species from the old literature (e.g. KREUTZ *et al.*, 2012) and finding of new ones.

According to FOKIN (2010), even though the composition of *Paramecium* species is largely well-known in Europe and North America, new morphological species are possibly waiting to be discovered as the fauna of ciliates in regions such as tropical Asia, South America, Antarctica and the Arctic are investigated (FOKIN *et al.*, 2004; FOKIN, 2010).

In the present study, we characterize a novel morphological species of *Paramecium*, herein named *Paramecium grohmannae* sp. nov., found in samples of water with activated sludge from a wastewater treatment plant in Rio de Janeiro, Brazil. The new species is described from light microscopy, and its phylogenetic affinities hypothesized from analyses of 18S-rDNA.

MATERIAL AND METHODS

Collection and Morphological Characterization

Specimens of *P. grohmannae* were obtained from samples of water with activated sludge collected from the primary decanter of Estação de Tratamento de Esgotos da Penha (ETE-Penha, CEDAE/RJ), a wastewater treatment plant located in the district of Penha, Rio de Janeiro, Brazil, in June of 2010. The organisms were kept in glass Petri dishes with ordinary limnetic cultures, made of small aliquots of the samples with addition of crushed rice grains to promote the growth of bacteria which serve as primary food source for the ciliates (e.g. FOISSNER *et al.*, 2002; PAIVA & SILVA-NETO, 2007). Additional

clonal cultures, used for DNA isolation, were made from single specimens.

Description was based on observation of live specimens under bright field, phase contrast and differential interference contrast (DIC) at 100× – 400× and 1,000× (oil immersion), and on protargol-impregnation following the protocol of DIECKMANN (1995). Measurements in Table 1 are in µm and were based on protargol-impregnated specimens (except for data on micronuclei) measured at 1,000×. Classification follows LYNN (2008), and terminology is mostly according to FOKIN (2010).

Isolation of DNA, PCR and Sequencing

About 50 specimens were isolated from clonal cultures, transferred to an embryo dish with mineral water and let starving overnight for about 16 hours. In the following day, the specimens were washed three times in mineral water and then fixed in sterile 70% ethanol for DNA extraction. The DNA was isolated using Purelink® Genomic DNA Mini Kit (Life Technologies), following manufacturer's instructions. Universal primers for Eukaryotes (F: 5'-AACCTGGTTGATCCTGCCAG-3'; R: 5'-GATCCTTCTGCAGGTTACCTAT-3') were used for PCR as described in PETRONI *et al.* (2000). The resulting gene fragments were purified using NucleoSpin® Gel and PCR Clean-up Kit (Macherey-Nagel), and sequenced in an ABI 3130 (Life Technologies) automatic sequencer.

Phylogenetic Analyses

The obtained 18S-rDNA sequence was analyzed altogether with 46 other sequences of *Paramecium* sampled from the NCBI/GenBank, emphasizing *P. multimicronucleatum* Powers and

Mitchell, 1910, which was the most similar to our isolate according to an initial BLAST (ALTSCHUL *et al.*, 1990) search. Two outgroup sequences, namely *Apofrontonia dohrni* Fokin *et al.*, 2006, and *Frontonia didieri* Long *et al.*, 2008, were included and analyzed simultaneously. Nucleotide alignment was performed with the MUSCLE algorithm implemented in MEGA 5.1 (TAMURA *et al.*, 2011), using default parameters, and further refined by eye. Overall *p*-distances in Table 2 were computed with MEGA 5.1, using pairwise deletion as treatment for gaps and missing data.

Phylogenetic analyses were ran under Bayesian inference (BI) and maximum likelihood (ML) frameworks, using the GTR + I (=0.6072) + G (=0.5265) nucleotide substitution model selected via the Akaike information criterion (AIC) (AKAIKE, 1974; BOS & POSADA, 2005) in MODELTEST 3.7 (POSADA & CRANDALL, 1998).

The BI was performed using the program MrBayes 3.2.2 implemented in CIPRES Science Gateway (MILLER *et al.*, 2010), and was based on two independent Markov Chain Monte Carlo (MCMC) simulations ran with four chains of 5,000,000 generations. Trees were sampled each 1,000 generations, and the first 25% of sampled trees were discarded as burn-in. For ML, the sequence matrix was analyzed with the program PhyML 3.0 (GUINDON *et al.*, 2010), starting from a BioNJ tree of which likelihood was improved via subtree pruning and regrafting (SPR) branch-swapping moves to achieve the ML tree.

Node stability in BI was assessed via posterior probabilities calculated from a 50% majority-rule consensus of trees retained after burn-in, and in ML, the SH-like aLRT branch support was used (ANISIMOVA & GASCUEL, 2006; SCHNEIDER, 2007; GUINDON *et al.*, 2010). In all trees, the root

was placed *a posteriori*, according to outgroup position (NIXON & CARPENTER, 1993).

RESULTS

Paramecium grohmannae sp. nov. (Table 1; Figures 1a–h, 2a–f)

Subphylum Intramacronucleata Lynn, 1996

Class Oligohymenophorea Puytorac *et al.*, 1974

Order Peniculida Fauré-Fremiet in Corliss, 1956

Family Parameciidae Dujardin, 1840

Genus *Paramecium* Müller, 1773

Diagnosis. Counterclockwise rotating freshwater *Paramecium* measuring in vivo ~180 x 65 µm (N = 10); body outline intermediate between “aurelia” and “bursaria” types; two (rarely three) contractile vacuoles, each with one excretion pore and usually nine long collecting canals; long outlet canals absent; buccal overture slight below body equator; macronucleus above body equator, ellipsoid to obovoid, measuring ~64 x 24 µm; one or two globular endosomal micronuclei ~5 µm in diameter with endosome ~2.5 µm.

Species name. In dedication to Prof. Dr. Priscila A. Grohmann, former scientific mentor of T. da S. Paiva during his early undergraduate period.

Type locality. Estação de Tratamento de Esgotos da Penha (ETE-Penha, CEDAE/RJ) Penha district, Rio de Janeiro – RJ, Brazil. Geographic coordinates: 22°50'00”S 43°16'03”W.

Deposition of type-specimens. Type slides (protargol-impregnation) of *P. grohmannae* were deposited in the collection of Laboratório de Protistologia, Dept. de Zoologia, Inst. de Biologia, Universidade Federal do Rio de Janeiro. Accession codes: IBZ-0007-2 – holotype (marked with ink on the slide) and paratypes; IBZ-0007-3 – paratypes.

The obtained 18S-rDNA fragment was deposited in the NCBI/GenBank under the accession code KJ755359.

Description. Specimens swim always rotating counterclockwise along major axis, staying most of the time in the water column; shape does not change when resting on bottom of Petri dishes. Outline intermediate between “aurelia” and “bursaria” forms, because live free-swimming specimens moderately flat anteriorly, with conspicuous preoral concavity, and obovate-tapered posteriorly. Body measuring 150–205 μm along longitudinal axis, slightly narrower at anterior region than close to posterior end, with largest width (39–78 μm) just below body equator. Usually two contractile vacuoles (rarely three), each having 7–10 (often nine) long collecting canals; single dorsal excretory pore per vacuole; long outlet canals absent (Figures 1a–e). Food vacuoles contained mostly bacteria;

cytoproct 20 μm long, located at $\sim 15 \mu\text{m}$ from rear end of body (Figure 2f).

Cortex with ordinary acerose to fusiform trichocysts measuring $\sim 5 \times 1 \mu\text{m}$ (undischarged) (Figure 1f); cytoplasm transparent beige with many $\sim 5 \mu\text{m}$ long refractive inclusions concentrated mostly near rear end, but also scattered inside body. Such inclusions appeared black under stereomicroscope (Figure 1a). Infundibulum curve, measuring 18–30 μm long, located just below body equator, with elliptical buccal overture at 78–98 μm from anterior end of body (Figures 1a, b, 2d); preoral suture inconspicuous (Figure 2e); oral cortex with a quadrulus and two peniculi (Figures 2a–c). Endoral not found, possibly due to insufficient impregnation. Somatic ciliature arranged in ~ 95 kineties bearing $\sim 7.5 \mu\text{m}$ long ordinary cilia plus a caudal tuft of $\sim 15 \mu\text{m}$ long cilia (Figure 1f).

Macronucleus located within anterior half

Table 1. Morphometric characterization of *Paramecium grohmannae* sp. nov.

Character ^a	Mean	M	SD	SE	CV(%)	Min	Max	N
Body length	171.4	172.5	9.7	1.4	5.7	150.0	205.0	50
Largest width of body	53.6	55.0	8.6	1.2	16.1	39.0	78.0	50
Distance from anterior end of body to equatorial region of oral overture	89.5	91.0	4.8	0.8	5.4	78.0	98.0	33
Length of oral overture	24.1	24.0	3.6	0.6	15.0	18.0	30.0	33
Length of macronucleus	63.8	60.0	9.9	1.8	15.6	40.0	90.0	31
Width of macronucleus	24.2	25.0	4.8	0.9	20.0	15.0	39.0	31
Number of micronuclei ^b	1.2	1.0	0.4	0.1	35.1	1	2	10
Diameter of micronuclei ^b	5.3	5.5	0.9	0.3	15.5	4.0	6.0	10
Diameter of endosome ^b	2.7	2.8	0.4	0.1	15.5	2.0	3.0	10

a CV – coefficient of variation; M – median; Max – maximum value observed; Mean – arithmetic mean; Min – minimum value observed; N – sample size; SD – standard deviation; SE – standard error.

b Data obtained from live specimens.

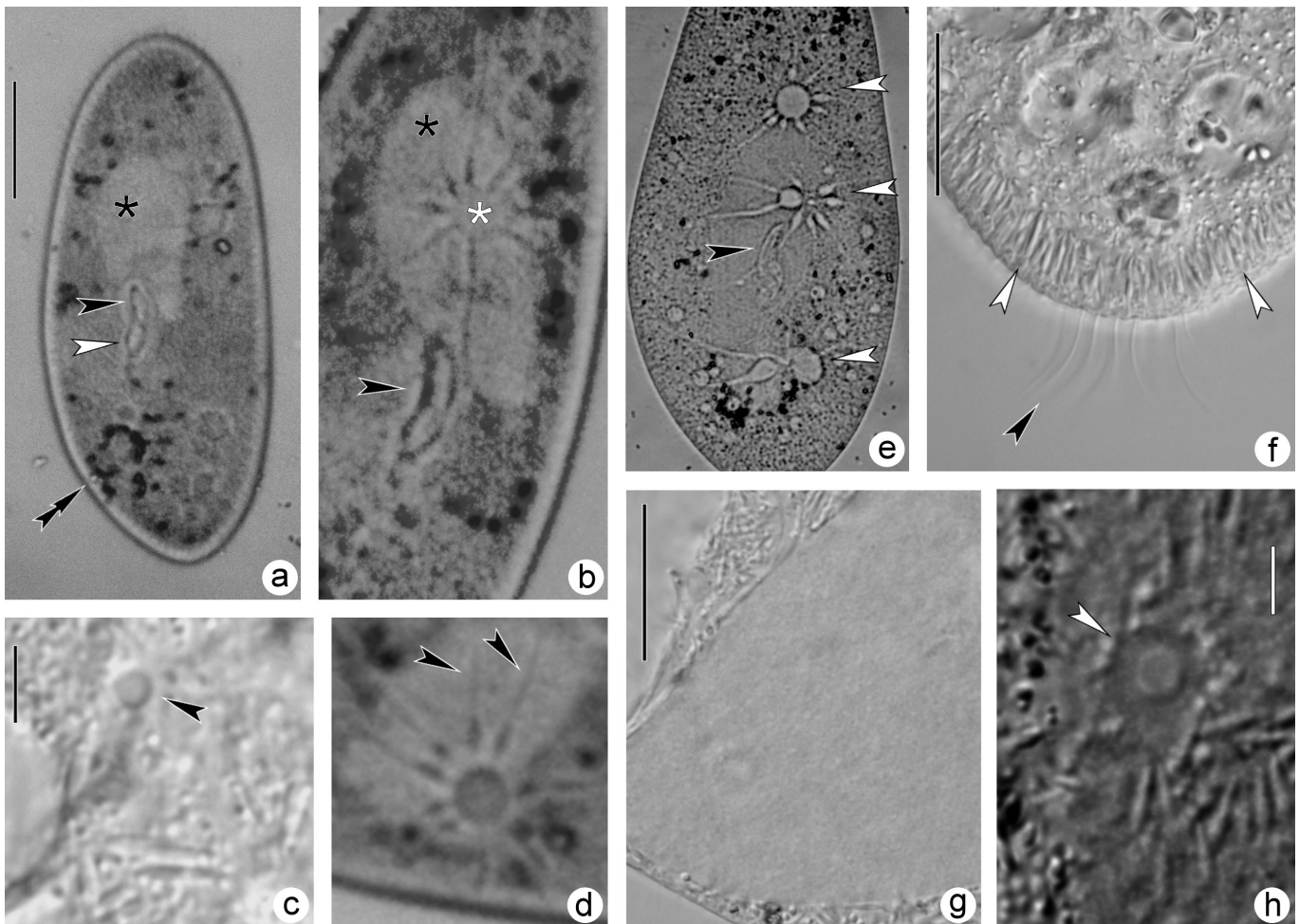


Figure 1. *Paramecium grohmannae* sp. nov. in vivo. a, b, d, e: Bright field; c, g–h: DIC. a: Live specimen showing position of cytostome and macronucleus (asterisk). Black arrowhead shows oral opening and white arrowhead indicates infundibulum. Double arrowheads show refractive cytoplasmic inclusions; b: Anterior contractile vacuole (white asterisk), macronucleus (black asterisk) and cytostome (arrowhead); c: Detail of contractile vacuole excretory pore (arrowhead); d: Contractile vacuole with collecting canals (arrowheads); e: Specimen with three contractile vacuoles (white arrowheads). Black arrowhead shows the cytostome; f: Detail of rear end of body showing caudal ciliary tuft (black arrowhead) and trichocysts below the pellicle (white arrowheads); g: Detail of smooth surface of macronucleus; h: Endosomal micronucleus (arrowhead) with endosome particle in the middle. Scale bars: a = 40 μm ; c, h = 4 μm ; f, g = 20 μm .

of body; ellipsoid to obovoid, measuring 40–90 x 15–39 μm (after protargol-impregnation), with smooth surface under DIC; interior with numerous chromatin condensations of ~ 1 μm in diameter (Figures 1a, b, g; 2a, d). Micronuclei not recognized in protargol-impregnated specimens, hence only studied in vivo. Usually one (less frequently two) globular endosomal (“type III” in FOKIN *et al.*, 2010) micronucleus of ~ 4 –6 μm in diameter,

always attached to macronucleus, with endosome diameter ~ 2 –3 μm (Figure 1h).

Molecular Phylogeny

The obtained 18S-rDNA fragment had 1,220 nt (without gaps) and a C + G content of 43.0 mol%. After the sequences were aligned, the matrix had a total of 1,775 characters, of which

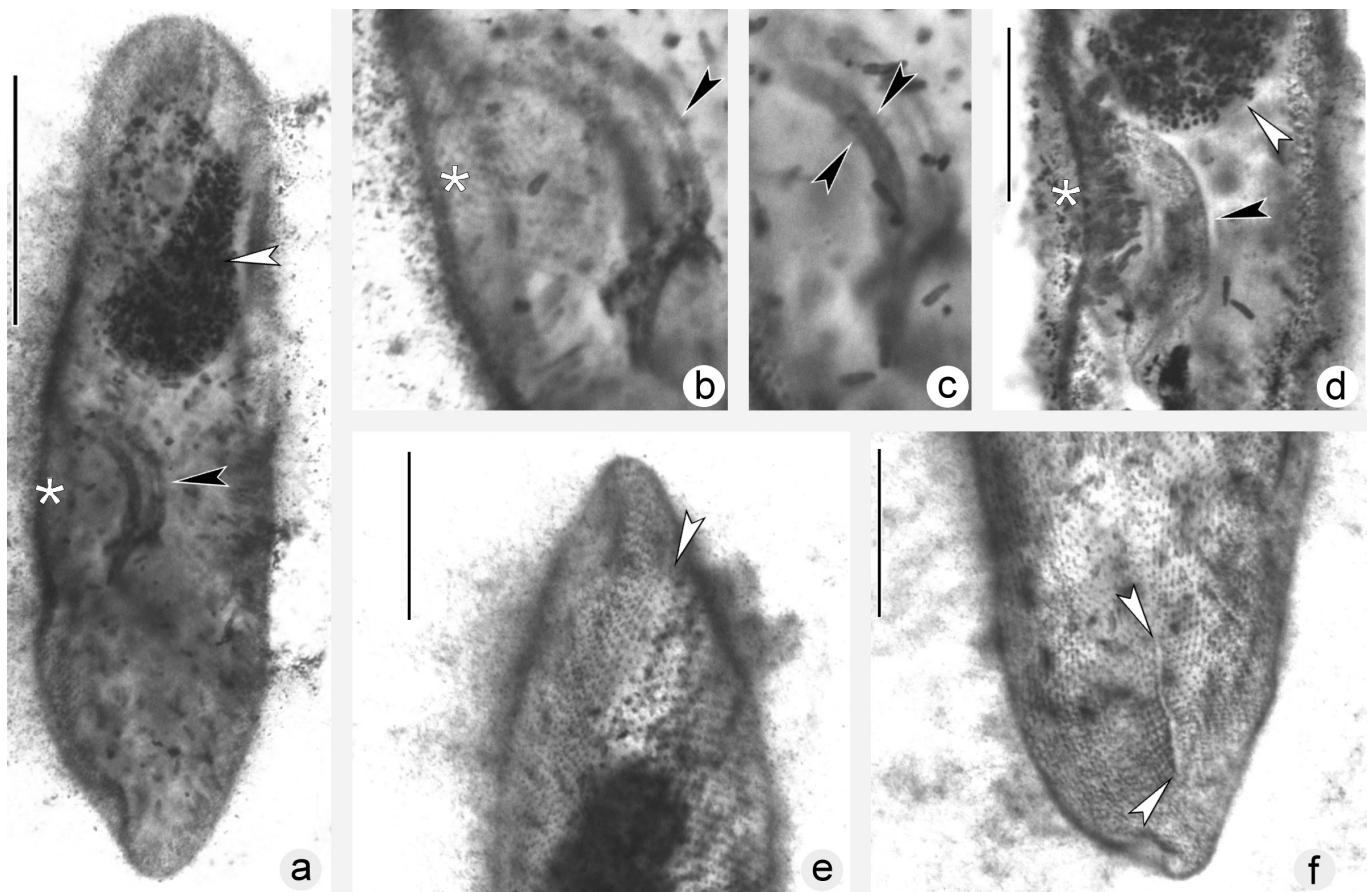


Figure 2. *Paramecium grohmannae* sp. nov. after protargol-impregnation. a, b, d: Holotype. a: Left side, showing position of oral cortex ciliature (black arrowhead) and macronucleus (white arrowhead); b: Detail of quadrulus (arrowhead); c: Detail of peniculi (arrowheads); d: Position of infundibulum (black arrowhead) in relation to macronucleus (white arrowhead); e: Ventral side, anterior region showing inconspicuous preoral suture (arrowhead); f: Ventral side, posterior region showing cytoproct (arrowheads). Asterisks in a, b, d indicate oral overture. Scale bars: a = 50 μ m; d–f = 25 μ m.

1,366 were constant. Since a small portion (6%) of the *P. grohmannae* sequence had uncertain nucleotide positions (coded as “N”), we performed an additional ML analysis removing those positions, and compared the resulting trees by eye, to see whether their inclusion would affect branch lengths or tree topology. Neither did happen.

Neither BI and ML results (Figure 3) rejected the monophyly of *Paramecium* in relation to the selected outgroup, and both were generally congruent in topology, with BI consensus slightly less resolved than the ML tree within the *Paramecium aurelia* complex cluster (SONNEBORN,

1975; AUFDERHEIDE *et al.*, 1983), and within each of the two major clusters of *P. multimicronucleatum*. Both analyses hypothesized three of the subgenera of *Paramecium* as monophyla, namely *Chloroparamecium* Fokin *et al.*, 2004, *Cypriostomum* Fokin *et al.*, 2004, and *Paramecium* Müller, 1773. *Helianter* Jankowski, 1969, was paraphyletic due to the ladderized branching pattern of *P. putrinum* Claparède and Lachman, 1858, and *P. duboscqui* Chatton and Brachon, 1933. The monophyly of *Viridoparamecium* Kreutz *et al.*, 2012, could not be tested because only one sequence of *P. chlorelligerum* Kahl, 1935, was available in the

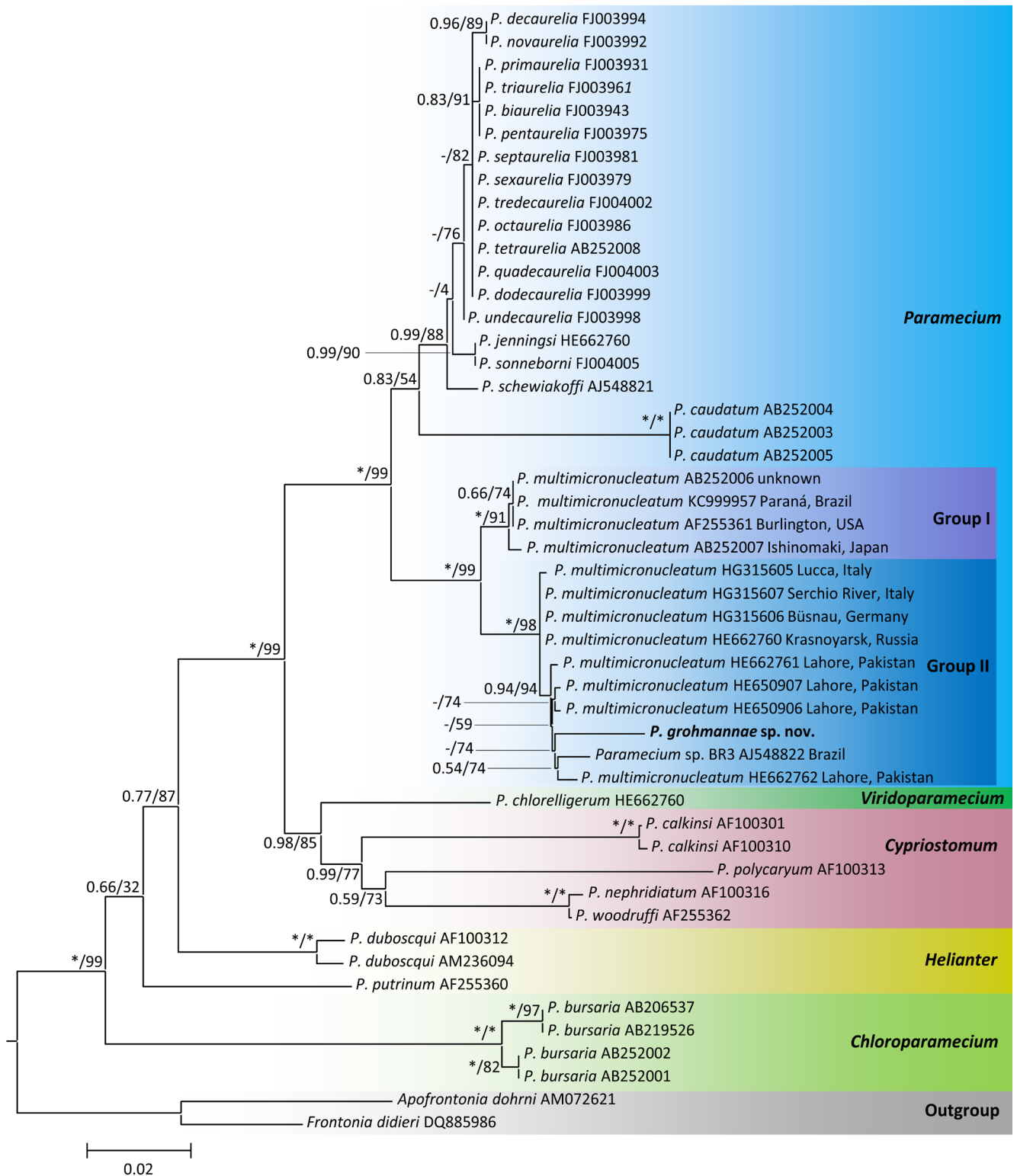


Figure 3. Maximum likelihood tree ($-\ln L = 7010.145204$) of genus *Paramecium* showing its subgenera and subdivision of *P. multimicronucleatum* in Groups I and II, with position of *P. grohmannae* sp. nov. NCBI/GenBank accession codes are given right of species names. Values associated to nodes are Bayesian posterior probabilities and SH-like aLRT support, respectively; * = full support; - = collapsed node in the BI consensus tree. Scale bar = two substitutions per 100 nucleotide positions.

NCBI/GenBank when the analyses were performed.

Paramecium grohmannae branched within the cluster of *P. multimicronucleatum*, which was the adelphotaxon of the cluster formed by *P. caudatum* Ehrenberg, 1833, + (*P. schewiakoffi* Fokin *et al.*, 2001, + *P. aurelia* complex). The *P. multimicronucleatum* cluster was consistently bifurcated, with strong data support (>90%; >0.90), distributing its representatives in two groups, herein named Group I and Group II, which were also strongly supported by the data. In results from both analyses, Group I included strains from Japan, USA and the south of Brazil, plus one sequence of which sampling site is unknown (see HOSHINA *et al.*, 2006). Group II included strains from Europe, Pakistan, and two from Brazil, including the one herein described as *P. grohmannae* sp. nov. In

the ML tree, which was slightly more resolved than the BI consensus, *P. grohmannae* was closely related to *P. multimicronucleatum* strain BR3, collected from Brazil (personal communication from S. Krenek), and a strain from Lahore, Pakistan, with moderate data support (>70%). A 18S-rDNA distance matrix of the terminals that constitute the *P. multimicronucleatum* cluster is shown in Table 2.

DISCUSSION

Comparison with Related Species

According to FOKIN (2010), using a combination of micronuclei and contractile vacuole characteristics is a promising way of species discrimination in *Paramecium*. The population herein described exhibits a unique combination

Table 2. 18S-rDNA distance matrix of the *Paramecium multimicronucleatum* cluster sequences (indicated by NCBI/GenBank access codes and sample origin), including *P. grohmannae* sp. nov.

Sequences	1	2	3	4	5	6	7	8	9	10	11	12	13
1 KJ755359 <i>P. grohmannae</i> sp. nov.													
2 AB252006 unknown	0.038												
3 AB252007 Ishinomaki, Japan	0.038	0.003											
4 AF255361 Burlington, USA	0.026	0.000	0.003										
5 AJ548822 "strain BR3", Brazil	0.014	0.022	0.024	0.021									
6 HE650906 Lahore, Pakistan	0.018	0.019	0.021	0.018	0.008								
7 HE650907 Lahore, Pakistan	0.019	0.020	0.021	0.018	0.008	0.002							
8 HE662760 Krasnoyarsk, Russia	0.004	0.038	0.038	0.038	0.008	0.004	0.008						
9 HE662761 Lahore, Pakistan	0.018	0.019	0.021	0.018	0.008	0.003	0.003	0.006					
10 HE662762 Lahore, Pakistan	0.021	0.022	0.024	0.021	0.009	0.006	0.006	0.014	0.006				
11 HG315605 Lucca, Italy	0.011	0.016	0.018	0.016	0.009	0.004	0.004	0.002	0.004	0.007			
12 HG315606 Bünsau, Germany	0.009	0.015	0.016	0.015	0.008	0.003	0.003	0.000	0.003	0.006	0.001		
13 HG315607 Serchio River, Italy	0.005	0.015	0.017	0.015	0.006	0.002	0.002	0.000	0.002	0.006	0.001	0.000	
14 KC999957 Paraná, Brazil	0.063	0.000	0.000	0.000	0.066	0.063	0.069	0.057	0.066	0.063	0.060	0.057	0.057

of such features, and therefore is regarded as a novel species, viz. *Paramecium grohmannae* sp. nov. Since it has micronuclei of the endosomal type, *P. grohmannae* is first compared with *P. calkinsi*, *P. duboscqui*, *P. nephridiatum* Gelei, 1925, and *P. woodruffi* Wenrich, 1928, which have micronuclei of the same kind (FOKIN, 1997, 2010).

In *P. calkinsi* and *P. duboscqui*, micronuclei are most of the times attached to macronucleus, which is similar to our finding. *Paramecium grohmannae* differs from *P. calkinsi* in number (on average one vs. 2–4) and diameter of micronuclei (4.0–6.0 μm vs. 1.7–3.4 μm); length of contractile vacuole collecting canals (long vs. short); and swimming rotation (always counterclockwise vs. preferably clockwise) (WOODRUFF, 1921; FOKIN, 1997; FOKIN, 2010). When compared with *P. duboscqui*, *P. grohmannae* differs in number (on average one vs. mostly two) and shape of micronuclei (globular vs. fusiform); structure of contractile vacuoles (with long collecting canals and one excretory pore vs. with collecting vesicles and short outlet canal); and swimming rotation (always counterclockwise vs. always clockwise) (CHATTON & BRACHON, 1933; FOKIN, 1997, 2010).

Paramecium nephridiatum has the macronucleus almost above oral overture level, which resembles *P. grohmannae*. However, its micronuclei, like in *P. woodruffi*, occur mostly free in the cytoplasm (vs. always attached to macronucleus in *P. grohmannae*). In addition, *P. grohmannae* also differs from *P. nephridiatum* in the number of micronuclei (on average one vs. three or four); and structure of contractile vacuole (with long collecting canals and one excretory pore vs. with short collecting canals and multiple pores). In comparison with *P. woodruffi*, *P. grohmannae* differs in number (on average one vs. 2–6) and diameter

of micronuclei (4.0–6.0 μm vs. 1.5–2.3 μm); and swimming rotation (always counterclockwise vs. easily changing rotation direction). Moreover, differently from *P. grohmannae*, body outline of the above compared species tend to be of the “bursaria” type, with *P. duboscqui* conspicuously curved outwards to the right (SERAVIN, 1970; FOKIN, *et al.*, 1999; FOKIN, 1997, 2010).

According to FOKIN (2010), some of the African species of *Paramecium*, namely *P. africanum* Dragesco, 1970, *P. jankowskii* Dragesco, 1972 and *P. pseudotrichium* Dragesco, 1979, may have endosomal micronuclei. However, those are of smaller diameter than the micronuclei of *P. grohmannae* (1.3–2.0 in *P. africanum*; 2.8–3.4 in *P. jankowskii*; 1.0–1.5 in *P. pseudotrichium*) (DRAGESCO, 1970; DRAGESCO, 1972). It is worthy of note that *P. africanum* has the oral overture placed slight below the equatorial level of body, which is similar to *P. grohmannae*, however it has conspicuously more micronuclei (4–9 vs. on average one in *P. grohmannae*), and a more prominent “aurelia” body outline (DRAGESCO, 1970). Contractile vacuoles of *P. pseudotrichium* have only three or four very short collecting canals (vesicles?), thus, according to FOKIN (2010), differing from all known congeners in which the vacuoles are canal-fed. Lastly, *Paramecium jankowskii* and *P. pseudotrichium* have pyriform and ellipsoid outlines, respectively, deviating from the typical morphotypes, including *P. grohmannae* (DRAGESCO, 1970; DRAGESCO & DRAGESCO-KERNÉIS, 1986; FOKIN, 2010).

Since our phylogenetic analyses have consistently placed *P. grohmannae* within the *P. multimicronucleatum* cluster, comparison with this latter becomes necessary. Most noticeable differences from strains of *P. multimicronucleatum* consist of nuclei features. Micronuclei of *P.*

grohmannae are conspicuously larger (4.0–6.0 μm vs. 0.7–2.3 μm) and less numerous (one; less frequently two vs. 2–5) than in typical *P. multimicronucleatum* (POWERS & MITCHELL, 1910; FOKIN, 1997; FOKIN & CHIVILEV, 2000). Additionally, micronuclei of *P. grohmannae* are of endosomal type, in which the organelle appears as a vesicle with a central compact and homogeneous mass (endosome), while *P. multimicronucleatum* has micronuclei of the vesicular type, in which the central mass appears toroidal under light microscope, because chromatin occupies only the periphery of nuclear volume (FOKIN, 1997, 2010). The macronucleus of *P. grohmannae* is located more anteriorly within the body and, on average, is more elongated than in *P. multimicronucleatum* (63.8 x 24.2 μm vs. 61.5 x 43.4 μm) (POWERS & MITCHELL, 1910; FOKIN & CHIVILEV, 2000). Nevertheless, the characteristics of contractile vacuoles in *P. grohmannae* are just as in *P. multimicronucleatum*, including the occurrence of specimens with three vacuoles (FOKIN, 2010).

Systematics of *Paramecium grohmannae* sp. nov.

The 18S-rDNA phylogenetic trees of *Paramecium* obtained in the present study are largely in agreement with the literature as it concerns the monophyletic condition and interrelationships of subgenera (e.g. STRÜDER-KYPKE *et al.*, 2000; FOKIN *et al.*, 2004; KREUTZ *et al.*, 2012), except *Helianter*, which sometimes is hypothesized as monophyletic (e.g. HOSHINA *et al.* 2006). The splitting of *P. multimicronucleatum* cluster in two major lineages with strong data support corroborates previous phylogenetic hypotheses based on ITS1-5.8S-rDNA-ITS2 and LSU-

rDNA (BARTH *et al.*, 2006; TARCZ *et al.*, 2012) and on the 18S-rDNA (BUOSI *et al.*, 2014), however slight different scenarios were hypothesized from COI mtDNA analyses, which displayed more resolution on the molecular intraspecific variation of *P. multimicronucleatum* (BARTH *et al.*, 2006; BOSCARO *et al.*, 2012; TARCZ *et al.*, 2012).

With exception of *P. caudatum*, syngens, i. e. cryptic or sibling species (LYNN, 2008), have been unveiled for all known species of *Paramecium*, with differences mostly at the molecular level, reflected at mating behavior (WICHTERMAN, 1986; TARCZ *et al.*, 2012). Within such context, *Paramecium multimicronucleatum* is a wide geographically distributed (FOKIN, 2010) complex of at least five syngens distinguishable via enzyme electrophoresis (ALLEN *et al.*, 1983a, b), which in so far did not receive Linnaean names, and according to FOKIN & CHIVILEV (2000), were never object of thorough morphometric investigation.

The phylogenetic pattern of the *P. multimicronucleatum* 18S-rDNA cluster, with a conspicuous bifurcation, in conjunct with the relatively long branches found in Group II suggest some strains in this cluster might have accumulated more changes over time than others (e.g. Group I). Hence, given its longest branch within Group II and the above discussed morphological differences from the original description of *P. multimicronucleatum*, *P. grohmannae* may be interpreted as a relatively highly apomorphic representative of the *P. multimicronucleatum* complex, having undergone sufficient morphological differentiation to be discernible at morphospecies level, and thus justifying the establishment of a new Linnaean name.

ACKNOWLEDGEMENTS

The authors are thankful to Maximiliano Dias da Silva de Moraes and Thiago Manchester de Mello for their technical support, and to the anonymous peer reviewers for their comments and suggestions. This study was financially supported by CNPq (Universal 014/2013, 485974/2013-4), FAPERJ (BIOTA E-26/110.022/2011), FAPESP (2015/17856-0) and European Commission FP7-PEOPLE-2009-IRSES project CINAR PATHOBACTER (247658).

REFERENCES

- AKAIKE, H.A. 1974. A new look at the statistical model identification. **IEEE Transactions on Automatic Control** **19**: 716-723.
- AL-SHAHWANI, S.M. & HORAN, N.J. 1991. The use of protozoa to indicate changes in the performance of activated sludge plants. **Water Research** **6**: 633-638.
- ALLEN, S.L.; NERAD, T.A. & RUSHFORD, C.L. 1983a. Comparison of the esterases and acid phosphatases in *Paramecium multimicronucleatum*, syngens 1-5, *P. jenningsi*, *P. caudatum*, and the *P. aurelia* complex. **Journal of Eukaryotic Microbiology** **30**: 148-154.
- ALLEN, S.L.; RUSHFORD, C.L.; NERAD, T.A. & LAU, E.T. 1983b. Intraspecific variability in the esterases and acid phosphatases of *Paramecium jenningsi* and *Paramecium multimicronucleatum*: assignment of unidentified paramecia; comparison with the *P. aurelia* complex. **Journal of Eukaryotic Microbiology** **30**: 155-163.
- ALTSCHUL, S.F.; GISH, W.; MILLER, W.; MYERS, E.W. & LIPMAN, D.J. 1990. Basic local alignment search tool. **Journal of Molecular Biology** **215**: 403-410.
- ANISIMOVA, M. & GASCUEL, O. 2006. Approximate likelihood ratio test for branches: A fast, accurate, and powerful alternative. **Systematic Biology** **55**: 539-552.
- AUFDERHEIDE, K.J.; DAGGETT, P.-M. & NERAD, T.A. 1983. *Paramecium sonneborni* n. sp., a new member of the *Paramecium aurelia* species-complex. **Journal of Protozoology** **30**: 128-131.
- BARTH, D.; KRENEK, S.; FOKIN, S.I. & BERENDONK, T.U. 2006. Intraspecific genetic variation in *Paramecium* revealed by mitochondrial cytochrome C oxidase I sequences. **Journal of Eukaryotic Microbiology** **53**: 20-25.
- BEALE, G.H. 1954. **The Genetics of *Paramecium aurelia***. Cambridge University Press, Cambridge. 178p.
- BEALE, G.H. & PREER-JR, J.R. 2008. ***Paramecium: Genetics and Epigenetics***. CRC Press, Boca Raton. 216p.
- BOS, D.H. & POSADA, D. 2005. Using models of nucleotide evolution to build phylogenetic trees. **Developmental & Comparative Immunology** **29**: 211-227.
- BOSCARO, V.; FOKIN, S.I.; VERNI, F. & PETRONI, G. 2012. Survey of *Paramecium duboscqui* using three markers and assessment of the molecular variability in the genus *Paramecium*. **Molecular Phylogenetics and Evolution** **65**: 1002-1013.
- BUOSI, P.R.; CABRAL, A.F.; SIMÃO, T.L.; UTZ, L.R. & VELHO, L.F. 2014. Multiple lines of evidence shed light on the occurrence of *Paramecium* (Ciliophora, Oligohymenophorea) in bromeliad tank water. **Journal of Eukaryotic Microbiology** **61**: 2-10.

- CHATTON, E. & BRACHON, S. 1933. Sur une paramécie a deux races: *Paramecium duboscqui* n. sp. **Compte Rendu Hebdomadaire des Séances et Mémoires de la Société de Biologie** **114**: 988-991.
- CURDS, C.R. 1992. **Protozoa and the water industry**. Cambridge University Press, Cambridge. 122p.
- CURDS, C.R. & COCKBURN, A. 1970. Protozoa in biological sewage treatment process. II Protozoa as indicators in the activated sludge process. **Water Research**. **4**: 237-249.
- DIECKMANN, J. 1995. An improved protargol impregnation for ciliates yielding reproducible results. **European Journal of Protistology** **31**: 372-382.
- DRAGESCO, J. 1970. Cilies libres du Cameroun. **Annales de la Faculté des Sciences, Yaoundé (Hors série)**: 1-141.
- DRAGESCO, J. 1972. Ciliés libres de l'Ouganda. **Annales de la Faculté des Sciences. Cameroun** **9**: 87-126.
- DRAGESCO, J. & DRAGESCO-KERNÉIS, A. 1986. Ciliés libres de l'Afrique intertropicale. Introduction à la connaissance et à l'étude des ciliés. **Faune tropicale** **26**: 1-559.
- FENCHEL, T. 1987. **The Ecology of the Protozoa: The Biology of Free-living Phagotrophic Protists**. Springer Verlag, New York. 197p.
- FOISSNER, W.; AGATHA, S. & BERGER, H. 2002. Soil ciliates (Protozoa, Ciliophora) from Namibia (Southwest Africa), with emphasis on two contrasting environments, the Etosha Region and the Namib Desert. **Denisia** **5**: 1-1459.
- FOKIN, S.I. 1997. Morphological diversity of the micronuclei in *Paramecium*. **Archiv für Protistenkunde** **148**: 375-387.
- FOKIN, S.I. 2010. *Paramecium* genus: biodiversity, some morphological features and the key to the main morphospecies discrimination. **Protistology** **6**: 227-235.
- FOKIN, S.I. & CHIVILEV, S.M. 2000. *Paramecium*. Morphometric analysis and taxonomy. **Acta Protozoologica** **39**: 1-14.
- FOKIN, S.I.; PRZYBOŚ, E.; CHIVILEV, S.M.; BEIER, C.L.; HORN, M.; SKOTARCZAK, D.; WODECKA, B. & FUJISHIMA, M. 2004. Morphological and molecular investigations of *Paramecium schewiakoffi* sp. nov. (Ciliophora, Oligohymenophorea) and current status of paramecia distribution and taxonomy. **European Journal of Protistology** **40**: 225-243.
- GÖRTZ, H.-D. 1988. **Paramecium**. Springer, Berlin. 444p.
- GUINDON, S.; DUFAYARD, J.F.; LEFORT, V.; ANISIMOVA, M.; HORDIJK, W. & GASCUEL, O. 2010. New algorithms and methods to estimate maximum-likelihood phylogenies: Assessing the performance of PhyML 3.0. **Systematic Biology** **59**: 307-321.
- HOSHINA, R.; HAYASHI, S. & IMAMURA, N. 2006. Intraspecific genetic divergence of *Paramecium bursaria* and reconstruction of paramecian phylogenetic tree. **Acta Protozoologica** **45**: 377-386.
- KREUTZ, M.; STOECK, M. & FOISSNER, W. 2012. Morphological and molecular characterization of *Paramecium* (*Viridoparamecium* nov. subgen.) *chlorelligerum* Kahl 1935 (Ciliophora). **Journal of Eukaryotic Microbiology** **59**: 548-563.
- LYNN, D.H. 2008. **The Ciliated Protozoa: Characterization, Classification and Guide to the Literature**, 3rd ed. Springer Press, New York. 608p.
- MILLER, M.A.; PFEIFFER, W. & SCHWARTZ, T. 2010. Creating the CIPRES Science Gateway for

- inference of large phylogenetic trees. In: **Proceedings of the Gateway Computing Environments Workshop**. IEEE, New Orleans, pp. 1-8.
- NIXON, K.C. & CARPENTER, J.M. 1993. On outgroups. **Cladistics 9**: 413-426.
- PAIVA, T.S. & SILVA-NETO, I.D. 2007. Morphology and morphogenesis of *Strongylidium pseudocrassum* Wang and Nie, 1935, with redefinition of *Strongylidium* Sterki, 1878 (Protista: Ciliophora: Stichotrichia). **Zootaxa 1559**: 31-57.
- PETRONI, G.; SPRING, S.; SCHLEIFER, K.H.; VERNI, F. & ROSATI, G. 2000. Defensive extrusive ectosymbionts of *Euplotidium* (Ciliophora) that contain microtubule-like structures are bacteria related to Verrucomicrobia. **Proceedings of the National Academy of Sciences USA 97**: 1813-1817.
- POSADA, D. & CRANDALL, K.A. 1998. Modeltest: Testing the model of DNA substitution. **Bioinformatics. 14**: 817-818.
- POWERS, J.H. & MITCHELL, C. 1910. A new species of *Paramecium* (*P. multimicronucleata*) experimentally determined. **Biological Bulletin 19**: 324-332.
- SCHNEIDER, H. 2007. **Métodos de Análise Filogenética - Um Guia Prático**. 3rd ed. SBG and Holos, Ribeirão Preto. 200p.
- SERAVIN, L.N. 1970. Left and right spiraling round the long body axis in ciliate protozoa. **Acta Protozoologica 7**: 312-323.
- SILVA, S.B.A. & SILVA-NETO, I.D. 2001. Morfologia dos protozoários ciliados presentes em um reator experimental de tratamento de esgoto pelo processo de lodos ativados. **Revista Brasileira de Zoociências 3**: 203-230.
- SONNEBORN, T.M. 1975. The *Paramecium aurelia* complex of fourteen sibling species. **Transactions of the American Microscopy Society 94**: 155-178.
- STRÜDER-KYPKE, M.C.; WRIGHT, A.D.; FOKIN, S.I. & LYNN, D.H. 2000. Phylogenetic relationships of the genus *Paramecium* inferred from small subunit rRNA gene sequences. **Molecular Phylogenetics and Evolution 14**: 122-130.
- TAMURA, K.; PETERSON, D.; PETERSON, N.; STECHER, G.; NEI, M. & KUMAR, S. 2011. MEGA5: Molecular Evolutionary Genetics Analysis using Maximum Likelihood, Evolutionary Distance, and Maximum Parsimony Methods. **Molecular Phylogenetics and Evolution 28**: 2731-2739.
- TARCZ, S.; POTEKHIN, A.; RAUTIAN, M. & PRZYBOŚ, E. 2012. Variation in ribosomal and mitochondrial DNA sequences demonstrates the existence of intraspecific groups in *Paramecium multimicronucleatum* (Ciliophora, Oligohymenophorea). **Molecular Phylogenetics and Evolution 63**: 500-509.
- VAN WAGTENDONK, W.J. 1974. **Paramecium. A Current Survey**. Elsevier Scientific Publishing Co., Amsterdam. 499p.
- WICHTERMAN, R. 1986. **The biology of Paramecium**. 2nd ed. Plenum Press, New York, London. 599p.
- WOODRUFF, L.L. 1921. The structure, life history, and intrageneric relationships of *Paramecium calkinsi* sp. nov. **Biological Bulletin 41**: 171-180.